Method of Moments (MoM): Application for Solving Augmented Electric Field Integral Equation (AEFIE)

By

Binye Li

Senior Thesis in Electrical Engineering

University of Illinois at Urbana-Champaign

Advisor: Weng Cho Chew

December 2014

Abstract

Surface integral equations (SIEs) are promising candidates for modeling circuits because they reduce degrees of freedom by restricting physical unknowns on the surface, which simplifies complex structures. However, there are still challenges related to achieving stability over a broad frequency band. Specifically, the low frequency breakdown of electrical field integral equation (EFIE) operator is discussed in this work. In order to solve or alleviate this problem, the separation of irrotational and solenoidal current must be accomplished. A proposed method, the Augmented Electrical Field Integral Equation (AEFIE), is intended to separate the current element by introducing charge as another variable and relate irrotational current and the charge vector. Finally, the method of moments (MoM) is applied to solve the integral equation by projecting the current onto RWG basis and performing subspace projections to fill out the integral equation operator matrix. For complicated circuit structure, MoM can be accelerated using the fast multipole algorithm (FMA).

Subject Keywords: ECE 499; Senior Thesis; Computational Electromagnetics; EFIE; MoM

Table of Contents

1. Introduction

The design of microelectronic devices is faced with many challenges, such as signal integrity, power integrity, electromagnetic interference, and so on. It is also not practical to put design into production before investigating the potential problems of such design. In order to know the flaws of a design beforehand, computational electromagnetics is the research area that provides accurate simulation result. Unlike traditional quasi-static methods, which neglects displacement current and focus on the problem in low frequency. Surface Integral Equation (SIE) method is going to give full wave electromagnetic analysis [3]. This project is going to focus on the challenges associated with this method and potential solutions.

2. Introduction to Electric Field Integral Equation (EFIE)

2.1 Electrical Field Wave Equation

It will be most intuitive to introduce Maxwell's equations before studying electromagnetic problems. The differential form of Maxwell's equations can be written as

$$\nabla \times \boldsymbol{E} = i\omega\mu \boldsymbol{H} \tag{2.1}$$

$$\nabla \times \boldsymbol{H} = -i\omega\varepsilon \boldsymbol{E} + \boldsymbol{J} \tag{2.2}$$

$$\nabla \cdot \varepsilon \boldsymbol{E} = \rho_e \tag{2.3}$$

$$\nabla \cdot \mu \boldsymbol{H} = 0 \tag{2.4}$$

In homogeneous media, the wave equation for the electrical field can be derived by taking the curl of Faraday's Law,

$$\nabla \times \nabla \times \boldsymbol{E} = i\omega\mu \nabla \times \boldsymbol{H} \tag{2.5}$$

and substituting with Ampere's Law,

$$\nabla \times \nabla \times \boldsymbol{E} = i\omega\mu(-i\omega\varepsilon \boldsymbol{E} + \boldsymbol{J}) = \omega^2 \mu\varepsilon \boldsymbol{E} + i\omega\mu \boldsymbol{J} \tag{2.6}$$

$$k^2 = \omega^2 \mu\varepsilon \tag{2.7}$$

As for homogeneous medium, the wave number is a constant. The wave equation of an electrical field with spatial dependence *r* is

$$\nabla \times \nabla \times \boldsymbol{E}(\boldsymbol{r}) - k^2 \boldsymbol{E}(\boldsymbol{r}) = i\omega\mu \boldsymbol{J}(\boldsymbol{r}) \tag{2.8}$$

2.2 The Dyadic Green's Function

The dyadic Green's function is the point source response to the vector wave equation [1]. The electric field can be formulized alternatively with the dyadic Green's function

$$\boldsymbol{E}(\boldsymbol{r}) = i\omega\mu \int_V d\boldsymbol{r}' \boldsymbol{J}(\boldsymbol{r}') \cdot \bar{G}(\boldsymbol{r}', \boldsymbol{r}) \tag{2.9}$$

Applying equation (2.9) to the wave equation derived in the last section, the following equation is achieved:

$$\nabla \times \nabla \times \bar{G}(\boldsymbol{r}) - k^2 \bar{G}(\boldsymbol{r}) = \bar{\mathrm{I}} \delta(\boldsymbol{r} - \boldsymbol{r}') \tag{2.10}$$

The right-hand side of this equation represents the point source. Mathematically, the solution [1] is given by

$$\bar{G}(\boldsymbol{r}) = (\bar{\mathrm{I}} + \frac{\nabla\nabla}{k^2}) \frac{e^{ik|\boldsymbol{r}-\boldsymbol{r}'|}}{4\pi|\boldsymbol{r}-\boldsymbol{r}'|} \tag{2.11}$$

Once the point source is known, the solution to the corresponding dyadic Green's function can be achieved by equation (2.11) [1]. Theoretically, the resulting electrical field distribution can be calculated when the current distribution and the point source response are given. In the next section, the equivalence principle is introduced to come up with the surface integral, and thus the electrical field integral equation (EFIE).

2.3 Equivalence Principle an Extinction Theorem

The setup for illustrating the Equivalence Principle and Extinction Theorem, according to [1], is shown in Figure 2-1

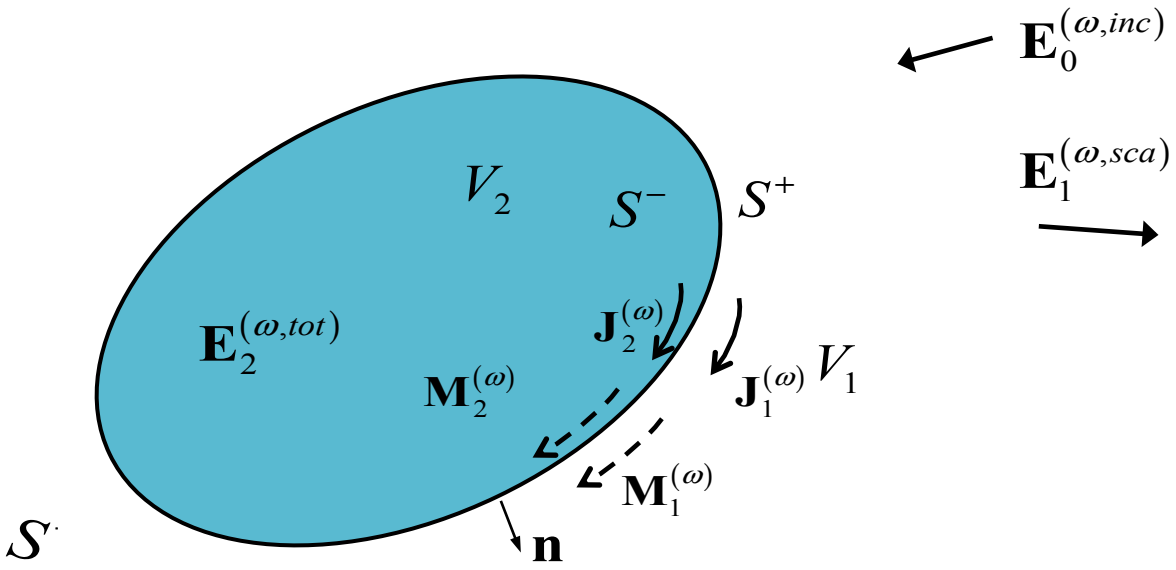

Figure 2-1 Equivalence Principle

$\mathbf{J}(\mathbf{r})$ represents the current $\mathbf{J}_1(\mathbf{r})$ and $\mathbf{J}_2(\mathbf{r})$, where $\mathbf{J}_1(\mathbf{r})$ is in V_1 and $J_2(\mathbf{r})$ is in V_2. Premultiplying equation (2.10) by E($\mathbf{r}$) and postmultiplying (2.8) by $\bar{\mathbf{G}}(\mathbf{r},\mathbf{r}')$, and then subtracting the resultant equations, the following equation is achieved:

$$\boldsymbol{E}(\boldsymbol{r})\cdot\nabla\times\nabla\times\bar{G}(\boldsymbol{r})-\nabla\times\nabla\times\boldsymbol{E}(\boldsymbol{r})\cdot\bar{G}(\boldsymbol{r})=\delta(\boldsymbol{r}-\boldsymbol{r}')\boldsymbol{E}(\boldsymbol{r})-i\omega\mu\boldsymbol{J}(\boldsymbol{r})\cdot\bar{G}(\boldsymbol{r}) \qquad (2.12)$$

and integrating the difference over the volume V_1

$$\begin{aligned}&\int_{V_1} dV[\boldsymbol{E}(\boldsymbol{r})\cdot\nabla\times\nabla\times\bar{G}(\boldsymbol{r})-\nabla\times\nabla\times\boldsymbol{E}(\boldsymbol{r})\cdot\bar{G}(\boldsymbol{r})]\\ &=\underbrace{\int_{V_1} d\boldsymbol{r}\,\delta(\boldsymbol{r}-\boldsymbol{r}')\boldsymbol{E}(\boldsymbol{r})}_{E(\boldsymbol{r}')}-i\omega\mu\underbrace{\int_{V_1} d\boldsymbol{r}\,\boldsymbol{J}_1(\boldsymbol{r})\cdot\bar{G}(\boldsymbol{r})}_{E_1(\boldsymbol{r}')}\end{aligned} \qquad (2.13)$$

The second term on the right-hand side of the equation shows that the field produced in V_1 comes from $\mathbf{J}_1$ only.

Using the identity that

$$\begin{aligned} &-\nabla\cdot[\boldsymbol{E}(\boldsymbol{r})\times\nabla\times\bar{G}(\boldsymbol{r},\boldsymbol{r}')+\nabla\times\boldsymbol{E}(\boldsymbol{r})\times\bar{G}(\boldsymbol{r},\boldsymbol{r}')] \\ &=\boldsymbol{E}(\boldsymbol{r})\cdot\nabla\times\nabla\times\bar{G}(\boldsymbol{r},\boldsymbol{r}')-\nabla\times\nabla\times\boldsymbol{E}(\boldsymbol{r})\cdot\bar{G}(\boldsymbol{r},\boldsymbol{r}') \end{aligned} \tag{2.14}$$

After applying Gauss's divergence theorem, the left hand side of the equation can be transformed into a surface integral.

$$\begin{aligned} &\boldsymbol{E}(\boldsymbol{r}')-\boldsymbol{E}_1(\boldsymbol{r}') \\ &=\oint_{S+S_{\text{inf}}} dS\ \ \hat{n}\cdot[\boldsymbol{E}(\boldsymbol{r})\times\nabla\times\bar{G}(\boldsymbol{r},\boldsymbol{r}')+\nabla\times\boldsymbol{E}(\boldsymbol{r})\times\bar{G}(\boldsymbol{r},\boldsymbol{r}')] \\ &=\oint_{S+S_{\text{inf}}} dS\ \ [\hat{n}\times\boldsymbol{E}(\boldsymbol{r})\cdot\nabla\times\bar{G}(\boldsymbol{r},\boldsymbol{r}')+i\omega\mu\hat{n}\times H(\boldsymbol{r})\cdot\bar{G}(\boldsymbol{r},\boldsymbol{r}')] \end{aligned} \tag{2.15}$$

The second step applied is to make use of Faraday's law. It can be argued that when the observation point **r'** is not within V_1, due to the sifting property of delta function involved in E_1, the above equation is formularized as

$$\boldsymbol{E}(\boldsymbol{r}')=\boldsymbol{E}_1(\boldsymbol{r}')+\oint_{S+S_{\text{inf}}} dS\ \ [\hat{n}\times\boldsymbol{E}(\boldsymbol{r})\cdot\nabla\times\bar{G}(\boldsymbol{r},\boldsymbol{r}')+i\omega\mu\hat{n}\times H(\boldsymbol{r})\cdot\bar{G}(\boldsymbol{r},\boldsymbol{r}')] \tag{2.16}$$

when the observation point is inside V_1, 0 otherwise.

$\mathbf{S}_{\text{inf}}$ refers to the infinite surface. The integrand in equation (2.16) decays as $1/\mathbf{r}$ as $\mathbf{r}$ goes to infinity [1]. The surface area grows at rate of $\mathbf{r}^2$. When integrated over, it seems it will result in some constant. However, the reality does not work as such. The leading terms of two operands cancel each other and leave us with higher order terms. Thus, the integration over $\mathbf{S}_{\text{inf}}$ will vanish. We use the reciprocity Theorem, which states that the dyadic Green's function is the same as its

transpose. The following can be shown with substitutions of the definitions of surface magnetic and electric currents, $\mathbf{M}_S$ and $\mathbf{J}_S$.

$$M_s(\boldsymbol{r}) = -\hat{n} \times E(\boldsymbol{r}), J_s(\boldsymbol{r}) = -\hat{n} \times H(\boldsymbol{r}) \tag{2.17}$$

$$\boldsymbol{E}(\boldsymbol{r}') = \boldsymbol{E}_1(\boldsymbol{r}') - \oint_S dS \ [\nabla \times \bar{G}(\boldsymbol{r}', \boldsymbol{r}) \cdot M_s(\boldsymbol{r}) - i\omega\mu \bar{G}(\boldsymbol{r}', \boldsymbol{r}) \cdot J_s(r)] \tag{2.18}$$

Switching **r** and **r'**, the formula becomes

$$\boldsymbol{E}(\boldsymbol{r}) = \boldsymbol{E}_1(\boldsymbol{r}) - \oint_S dS \ [\nabla \times \bar{G}(\boldsymbol{r}, \boldsymbol{r}') \cdot M_s(\boldsymbol{r}') - i\omega\mu \bar{G}(\boldsymbol{r}, \boldsymbol{r}') \cdot J_s(\boldsymbol{r}')] \tag{2.19}$$

The physical picture above is as follows: The total **E** field consists of two parts. The first contribution is the current density J1 inside V1. The second contribution is current J2 and any other source inside V2, which is equivalently the magnetic current and electric current on the surface S.

Furthermore, when the observation point is in V2, the electric field will be zero. Fields from the source in region 1 cancel those in region 2. This is known as the *extinction theorem*.

The core idea of the equivalence principle is to create a free space, in which there is a surface containing magnetic and electric current. These equivalent current sources act as source to the scattering field in the region [1]. The region where the original dielectric is positioned has zero fields.

To extract the EFIE from the above equation, a simple example of a perfect electric conductor (PEC) is introduced.

2.4 EFIE-Perfect Electric Conductor

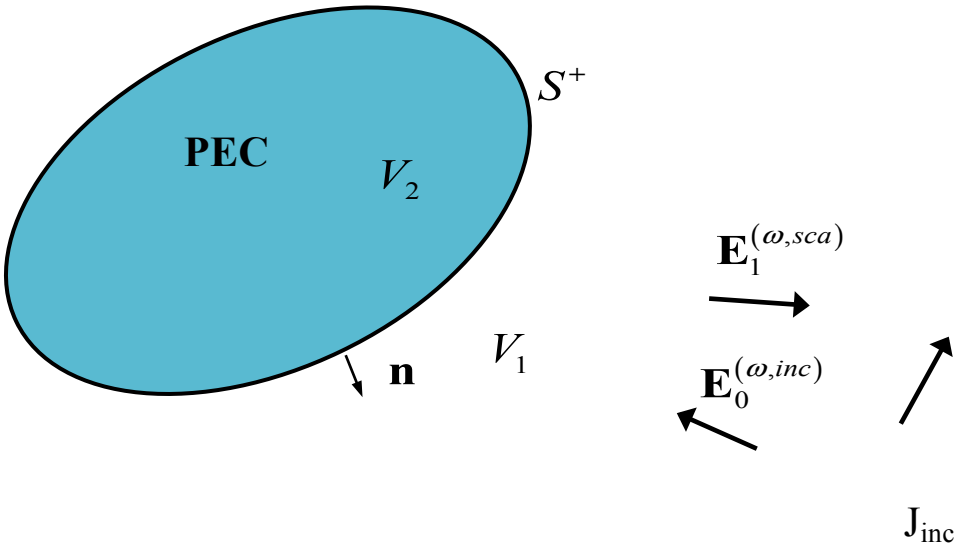

Figure 2-2 Scattering by a PEC object

For a PEC object, as demonstrated in [1], no field will be produced inside. The electric field from outside towards the surface will be perpendicular to the surface, leading to

$$M_{eq} = E \times \hat{n} = 0 \tag{2.20}$$

Then equation (2.19) becomes

$$\boldsymbol{E}(\boldsymbol{r}) = \boldsymbol{E}_{inc}(\boldsymbol{r}) + \oint_{S^+} dS \;\; i\omega\mu \bar{G}(\boldsymbol{r},\boldsymbol{r}') \cdot J_s(\boldsymbol{r}') \tag{2.21}$$

where E_1 represents the incident wave and the integral captures the scattered field in region V1. If taking the cross product between normal vector and the above equation, the focused region is the surface separating V1 and V2. For modes on surface S, it must be satisfied that the tangential component is 0 by continuity across the PEC boundary. Thus, the electric field integral equation (EFIE) is finally formularized as

$$\boldsymbol{E}(\boldsymbol{r}) = 0 = \hat{n} \times \boldsymbol{E}_{inc}(\boldsymbol{r}) + i\omega\mu\hat{n} \times \int_S dS' \quad \bar{G}(\boldsymbol{r}, \boldsymbol{r}') J_{eq}(\boldsymbol{r}') \tag{2.22}$$

3. Low Frequency Breakdown of EFIE

3.1 Example of Low Frequency Breakdown

The electrical field integral equation is used to solve problems computationally, which results in problems from the limited precision of computer.

The following results are from a typical computer program that utilizes EFIE to calculate RCS of a unit sphere with changes in theta. They are compared with results from calculation of the MIE series. The following two figures, figure 3-1 and 3-2, are simulated using existing code written by Hui Gan.

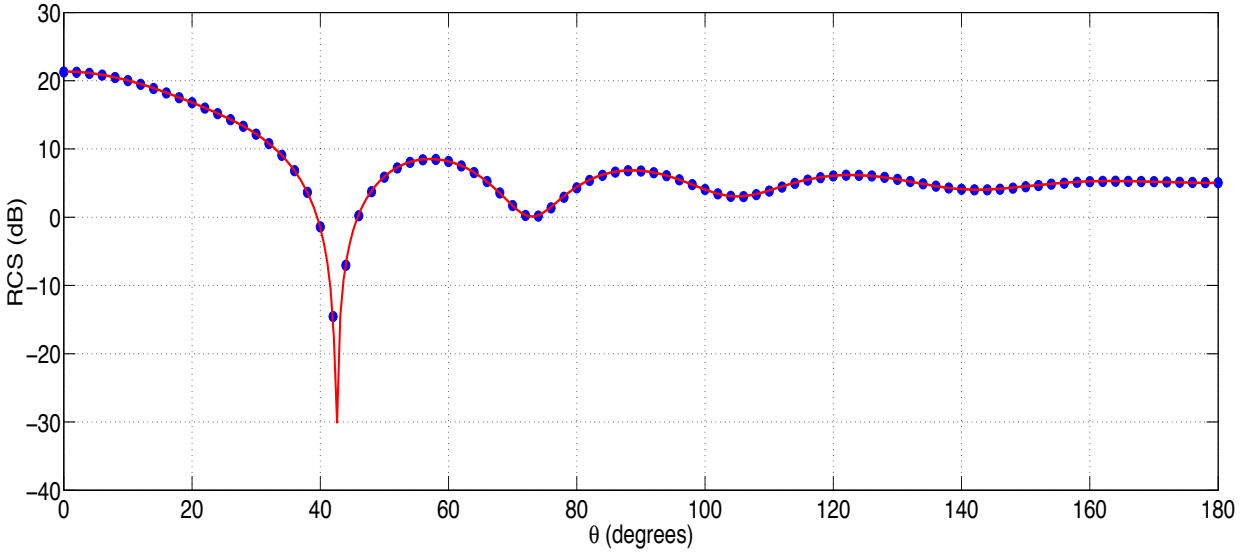

Figure 3-1 RCS vs. Theta at high frequency f=300MHz

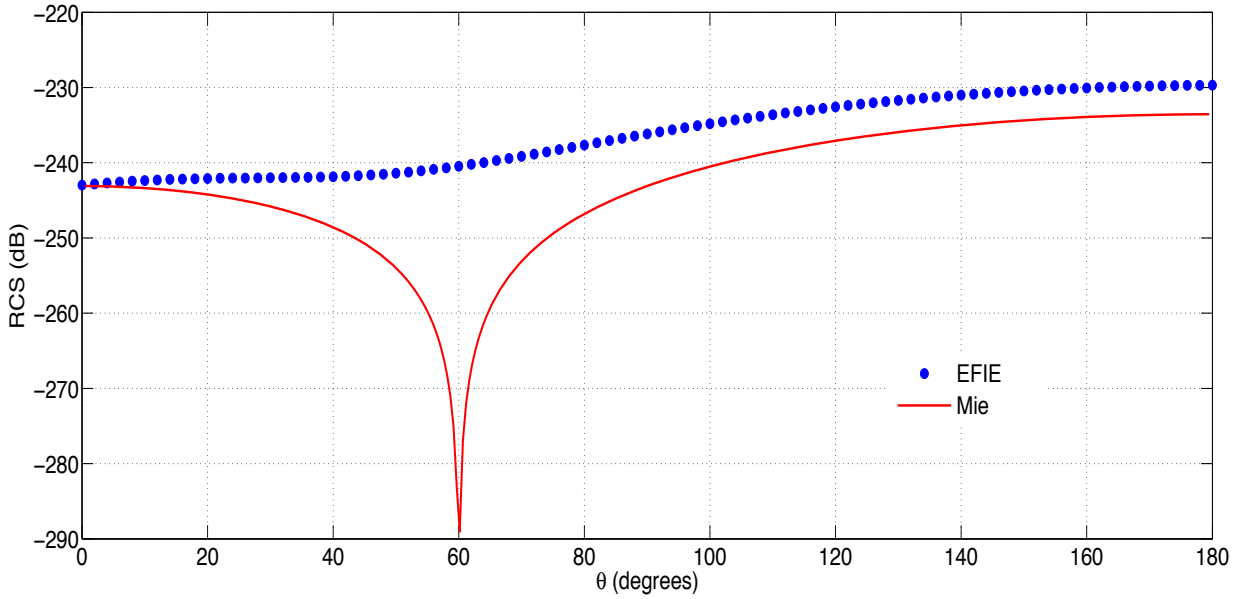

Figure 3-2 RCS vs. Theta at low frequency f=30Hz

The red curve represents the RCS value that is calculated from the MIE series while the blue dots are samples calculated using the electrical field integral equation. A match between the two methods can be identified when the frequency is high. However, significant differences are shown at low frequency. Three illustrations of the low frequency breakdown are discussed below.

3.2 Electromagnetic Equation when ω goes to 0

The current source is first decomposed into two parts:

$$J = J_{sol} + J_{irr} \tag{3.1}$$

J_{sol} is the solenoidal part, which is divergence free. J_{irr} is the irrotational part, which is curl free. This is known as the Helmholtz decomposition. According to the current continuity equation in frequency domain,

$$\nabla \cdot J = i\omega\rho_e \tag{3.2}$$

When frequency ω approaches 0, the equation for Gauss's law, equation (2.3), becomes

$$\nabla \cdot \varepsilon \boldsymbol{E} = \rho_e = \lim_{\omega->0} \frac{\nabla \cdot J}{i\omega} \tag{3.3}$$

The divergence of current source here must be approaching 0 or the term to the right hand side is unbounded. This current source corresponds to the J_{irr} because J_{sol} is divergence free. Hence, for extreme low frequency, it is safe to conclude that

$$\left|J_{sol}\right| << \left|J_{irr}\right| \tag{3.4}$$

Although the solenoidal component of the current density is much less than the irrotational component, the former cannot be neglected during computation. As noted from equation (3.3), the irrotational component of current contributes to the charge and electrical field, which is important for characterizing capacitor models. Meanwhile, the solenoidal component contributes to the magnetic field, which in turn describes the behavior of inductor models. When performing numerical calculation at low frequency, the solenoidal component might not be captured due to the limitation of computer precision [2].

3.3 Low Frequency Behavior of EFIE Operator

The dyadic Green's function can be written as

$$\bar{G}(\mathbf{r},\mathbf{r}') = (\bar{\mathrm{I}} + \frac{\nabla\nabla}{k^2}) g(\mathbf{r},\mathbf{r}') \tag{3.5}$$

Substituting into equation (2.22), after doing integration by parts once, the EFIE operator can be

identified as

$$\mathcal{L}_E \mathbf{J}_s = i\omega\mu \int_S d\mathbf{r}' g(\mathbf{r},\mathbf{r}') \mathbf{J}_s(\mathbf{r}') - \frac{1}{i\omega\varepsilon} \nabla \int_S d\mathbf{r}' g(\mathbf{r},\mathbf{r}') \nabla' \cdot \mathbf{J}(\mathbf{r}') \tag{3.6}$$

(1) (2)

The current density itself will produce a magnetic field from Ampere's law. In order words, the first integration corresponds to the electrical field generated by the oscillation of magnetic field. Meanwhile, the divergence of current density, from the continuity equation, corresponds to the idea of moving charges. Thus, the second integration describes the electrical field created by changes in the system.

As ω approaches 0, term (2) is going to dominate the equation. Such that

$$\mathcal{L}_E \mathbf{J}_s \simeq \frac{1}{i\omega\varepsilon} \nabla \int_S d\mathbf{r}' g(\mathbf{r},\mathbf{r}') \nabla' \cdot \mathbf{J}(\mathbf{r}') \tag{3.7}$$

In a real circuit, the surface current can be irrotational, solenoidal or a mixture. Thus there exists a surface current J_s such that its divergence is zero, namely $J_s=J_{sol}$. In this case, the eigenvalue for the EFIE operator will be extremely small. The approximated equation (3.7) is at a null space. On the other hand, there exists a surface current involving irrotational current such that the corresponding eigenvalue will be extremely large. Such physical response will make the matrix representation of EFIE operator ill-conditioned when frequency is low [2].

3.4 Low Frequency Behavior of wave equation

Solving Maxwell's equations to get the wave equation with current source,

$$\nabla \times \mu^{-1} \nabla \times \mathbf{E} - \omega^2 \varepsilon \mathbf{E} = i\omega \mathbf{J} \tag{3.8}$$

At low frequency, the second term vanishes, and the equation left is in the form of

$$\nabla \times \mu^{-1} \nabla \times \mathbf{E} \simeq i\omega \mathbf{J} \tag{3.9}$$

This is equivalent to

$$\nabla \times \mathbf{A} = \mathbf{b} \tag{3.10}$$

Equation (3.10) does not have a unique solution because adding a curl-free component to **A** will still satisfy the equation [2]

$$\nabla \times (\mathbf{A} + \nabla \phi) = \mathbf{b} \tag{3.11}$$

Mathematically, the matrix system is badly conditioned and involves infinite number of correct solutions while the real system should only have one valid answer.

3.5 Low Frequency Limit

It is necessary to study the low frequency limit, beyond which the breakdown of EFIE does not occur. Intuitively, the low frequency limit should be related to the size of the basis function. When the frequency is low and wavelength is large, the wave transmits as if the basis patch is invisible [3]. The reason for this is that the wavelength is much larger than the size of the basis,

so that the information of the basis function is hardly seen by the wave. Due to the finite computational precision, only large values can be collected and the smooth part of the EFIE matrix is hard to obtain.

4. Formulation of Augmented Electric Field Integral Equation (AEFIE)

4.1 Motivation

Full-wave electromagnetic modeling of microelectronic structure is an important method to predict the functionality of a design. It is better than the quasi-static method as the latter is not accurate at high frequencies. EFIE is one of the full-wave modeling techniques that covers a wide frequency band. However, a problem arises due to the low frequency breakdown described in the previous section. The main reason for the occurrence of low frequency breakdown is the limitation of computer memory, which cannot distinguish vector and scalar potentials at low frequency. In order to eliminate the low frequency problem, many techniques are implemented to separate the calculation involving vector and scalar potentials. The loop-tree method is one of them. However, the implementation of this method consumes a lot of memory to search for specific loops and trees, which is not practical for large-scale structures [3]. The augmented electric field integral equation includes charges as an extra parameter, which separates the contributions of the vector and scalar potential. In addition to that, an appropriate scaling method should be applied to account for precision limitation of computations in order to prevent from low frequency breakdown [2].

4.2 Rao-Wilton-Glisson Basis

RWG basis is widely used as the basis function to calculate full-wave scattering problems in microwave circuit simulations. The setup for the basis function is illustrated in the figure 4-1 as demonstrated in [1].

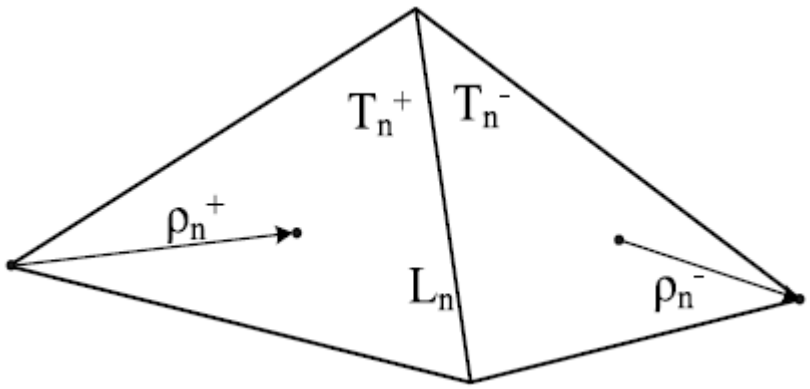

Figure 4-1 RWG basis function/element.

The basis function is defined as

$$\Lambda_n(\mathbf{r}) = \frac{l_n}{2A_n^{\pm}}\boldsymbol{\rho}_n^{\pm}(\mathbf{r}), \quad \mathbf{r} \in T_n^{\pm} \tag{3.12}$$

The superscripts + and – indicate the positive triangle and negative triangle. A_n defines the area of the n^{th} triangle. The term ρ_n , accordingly, is the vector inside the n^{th} RWG basis connecting the location r and the left or right tip of the triangle, depending on the choice of patch in the RWG basis [3].

For simplicity, for computing large scale problems, the basis function is normalized and simplified as

$$\Lambda_n(\mathbf{r}) = \begin{cases} \dfrac{\mathbf{r}-\mathbf{r}^+}{2A_n^+}, & \mathbf{r} \in T_n^+ \\ \dfrac{\mathbf{r}-\mathbf{r}^-}{2A_n^-}, & \mathbf{r} \in T_n^- \\ 0, \quad , & elsewhere \end{cases} \tag{3.13}$$

4.3 Formulation of RWG-based Integral Equation with Current Continuity

We define vector potential to be **V**, scalar potential to be **S** and pulse response to be **P**. These are all MoM matrix, which will be discussed in the next chapter. Then the matrix representations of these three parameters, using the method of moments (MoM), are written as

$$\left[\overline{\mathbf{V}}\right]_{m,n} = \mu_r \int_{S_m} \Lambda_m(\mathbf{r}) \cdot \int_{S_n} g(\mathbf{r},\mathbf{r}')\Lambda_n(\mathbf{r}')dS'dS \tag{3.14}$$

$$\left[\overline{\mathbf{S}}\right]_{m,n} = \varepsilon_r^{-1} \int_{S_m} \nabla\cdot\Lambda_m(\mathbf{r}) \cdot \int_{S_n} g(\mathbf{r},\mathbf{r}')\nabla'\cdot\Lambda_n(\mathbf{r}')dS'dS \tag{3.15}$$

$$\left[\overline{\mathbf{P}}\right]_{m,n} = \varepsilon_r^{-1} \int_{T_m} h_m(\mathbf{r}) \cdot \int_{T_n} g(\mathbf{r},\mathbf{r}')h_n(\mathbf{r}')dS'dS \tag{3.16}$$

These matrices can be interpreted as an operator that operates on the induced current on the surface, and the result is the excitations given. Revisiting equation (2.22), the matrix form for EFIE can be written as

$$(ik_0\eta_0\overline{\mathbf{V}} + \frac{\eta_0}{ik_0}\overline{\mathbf{S}})\cdot\mathbf{J} = \mathbf{b} \tag{3.17}$$

J is a vector that contains the current coefficient when projected on the RWG basis and **b** is the coefficient of the excitation given on the RWG basis. The definition of incidence matrix is further introduced as

$$\left[\overline{\mathrm{D}}\right]_{\mathrm{m,n}}=\begin{cases}0,\text{Patch m does not belong to RWG n}\\1,\text{Patch m is the positive part of RWG n}\\-1,\text{Patch m is the negative part of RWG n}\end{cases} \tag{3.18}$$

The incidence matrix is ideally a divergence operator. Using the incidence matrix, by which the positive flow of RWG basis is defined, the scalar potential can be further factorized as

$$\overline{\mathbf{S}}=\overline{\mathbf{D}}^{T}\cdot\overline{\mathbf{P}}\cdot\overline{\mathbf{D}} \tag{3.19}$$

The P matrix discretizes the charge. Through basis transformation, the scalar potential is found. For A-EFIE, the current continuity condition yields

$$\overline{\mathbf{D}}\cdot\mathbf{J}=ik_0c_0\boldsymbol{\rho} \tag{3.20}$$

c_0 is the speed of light in the medium. Combining equation (4.4), (4.6) and (4.7), the matrix form of A-EFIE using continuity of current is written as

$$\begin{pmatrix}\overline{\mathbf{V}} & \overline{\mathbf{D}}^{T}\cdot\overline{\mathbf{P}}\\ \overline{\mathbf{D}} & k_0^2\overline{\mathbf{I}}\end{pmatrix}\cdot\begin{pmatrix}ik_0\mathbf{J}\\ c_0\boldsymbol{\rho}\end{pmatrix}=\begin{pmatrix}\eta_0^{-1}\mathbf{b}\\ 0\end{pmatrix} \tag{3.21}$$

4.4 A-EFIE Formulation with Charge Neutrality

The above equation (4.8) still has low frequency deficiency. The physical reason for this is that the current continuity still contains the dynamic charge flow. Irrotational and solenoidal currents are not distinguished. In order to fully separate these two terms and ensure full rank down to DC, charge neutrality is introduced.

The first argument is made that the objects are composed of disconnected objects. Each object is isolated from the others. Thus the total charge within the object must be 0 to satisfy the charge

neutrality condition. $\boldsymbol{\rho}_{\mathrm{r}}$ is introduced to represent the vector of charges in reduced form. The forward matrix and backward matrix are defined to map the transformation between $\boldsymbol{\rho}_{\mathrm{r}}$ and $\boldsymbol{\rho}$.

$$\begin{aligned} \boldsymbol{\rho}_r &= \overline{\mathbf{F}} \cdot \boldsymbol{\rho} \\ \boldsymbol{\rho} &= \overline{\mathbf{B}} \cdot \boldsymbol{\rho}_r \end{aligned} \tag{3.22}$$

Then in the equation (4.8), the total charge is replaced with changes inside each spanning tree. The Augmented EFIE formulation is modified as

$$\begin{pmatrix} \overline{\mathbf{V}} & \overline{\mathbf{D}}^T \cdot \overline{\mathbf{P}} \cdot \overline{\mathbf{B}} \\ \overline{\mathbf{F}} \cdot \overline{\mathbf{D}} & k_0^2 \overline{\mathbf{I}_r} \end{pmatrix} \cdot \begin{pmatrix} ik_0 \mathbf{J} \\ c_0 \boldsymbol{\rho}_r \end{pmatrix} = \begin{pmatrix} \eta_0^{-1} \mathbf{b} \\ 0 \end{pmatrix} \tag{3.23}$$

5. Method of Moments (MoM) in A-EFIE

MoM solves integral form of Maxwell's equations. The unknowns of MoM are the equivalent electric current elements projected on the RWG basis.

For large-scale problems, usually it is hard to directly solve the scattering field and equivalent current on the surface. The method of moment introduces the idea of subspace projection, which results in another name for MoM, the subspace projection method. For example, if the formularized equation in matrix form is given by

$$\begin{pmatrix} a_{11} & \cdots & a_{1n} \\ \vdots & \ddots & \vdots \\ a_{m1} & \cdots & a_{mn} \end{pmatrix} = \begin{pmatrix} b_{11} & \cdots & b_{1n} \\ \vdots & \ddots & \vdots \\ b_{m1} & \cdots & b_{mn} \end{pmatrix} \tag{4.1}$$

then the fundamental idea of MoM is to solve the following:

$$\begin{pmatrix} a_{11} & \cdots & a_{1n} \\ \vdots & \ddots & \vdots \\ a_{m1} & \cdots & a_{mn} \end{pmatrix} \begin{pmatrix} v_1 \\ . \\ . \\ v_n \end{pmatrix} = \begin{pmatrix} b_{11} & \cdots & b_{1n} \\ \vdots & \ddots & \vdots \\ b_{m1} & \cdots & b_{mn} \end{pmatrix} \begin{pmatrix} v_1 \\ . \\ . \\ v_n \end{pmatrix} \tag{4.2}$$

Equation (5.2) does not directly imply equation (5.1), while using equation (5.2) will help filling in the matrix elements of the unknowns.

In the previous section, we mentioned the usage of MoM in these three equations:

$$\left[\overline{\mathbf{V}}\right]_{m,n} = \mu_r \int_{S_m} \Lambda_m(\mathbf{r}) \cdot \int_{S_n} g(\mathbf{r},\mathbf{r}')\Lambda_n(\mathbf{r}')dS'dS \tag{4.3}$$

$$\left[\overline{\mathbf{S}}\right]_{m,n} = \varepsilon_r^{-1} \int_{S_m} \nabla\cdot\Lambda_m(\mathbf{r}) \cdot \int_{S_n} g(\mathbf{r},\mathbf{r}')\nabla'\cdot\Lambda_n(\mathbf{r}')dS'dS \tag{4.4}$$

$$\left[\overline{\mathbf{P}}\right]_{m,n} = \varepsilon_r^{-1} \int_{T_m} h_m(\mathbf{r}) \cdot \int_{T_n} g(\mathbf{r},\mathbf{r}')h_n(\mathbf{r}')dS'dS \tag{4.5}$$

Equations (5.3)~(5.4) utilize the method of moments to calculate vector potential and Scalar potential by projecting the EFIE operator onto the RWG basis [1]. Equation (5.5) uses the projection of the capacitive term in the EFIE operator onto the pulse function basis in order to separate the irrotational and solenoidal terms.

6. Design of Graphical User Interface

6.1 Specification of Graphical User Interface

A graphical user interface (GUI) is designed to implement the functionality of computing electromagnetic problems. Problems are described in the form of Augmented electric field integral equation (AEFIE) and solved using method of moments (MoM).

The GUI is proposed to have the following functionality:

1) Creating project folder in the directory specified by the user
2) Creating three-dimensional view of the input mesh file
3) Generating parameter file according to user's input to the interface
4) Compiling and running the program with input files in the project folder automatically
5) Showing results in plots from the output data according to the output files

The GUI is developed using C++ language under Linux environment. It can be executable cross platform with minor modifications. Qwt and Qt packages are used to functionalize the GUI. Source codes are included in Appendix A.

Screenshots of the interface window are shown in Figure 6-1 and 6-2.

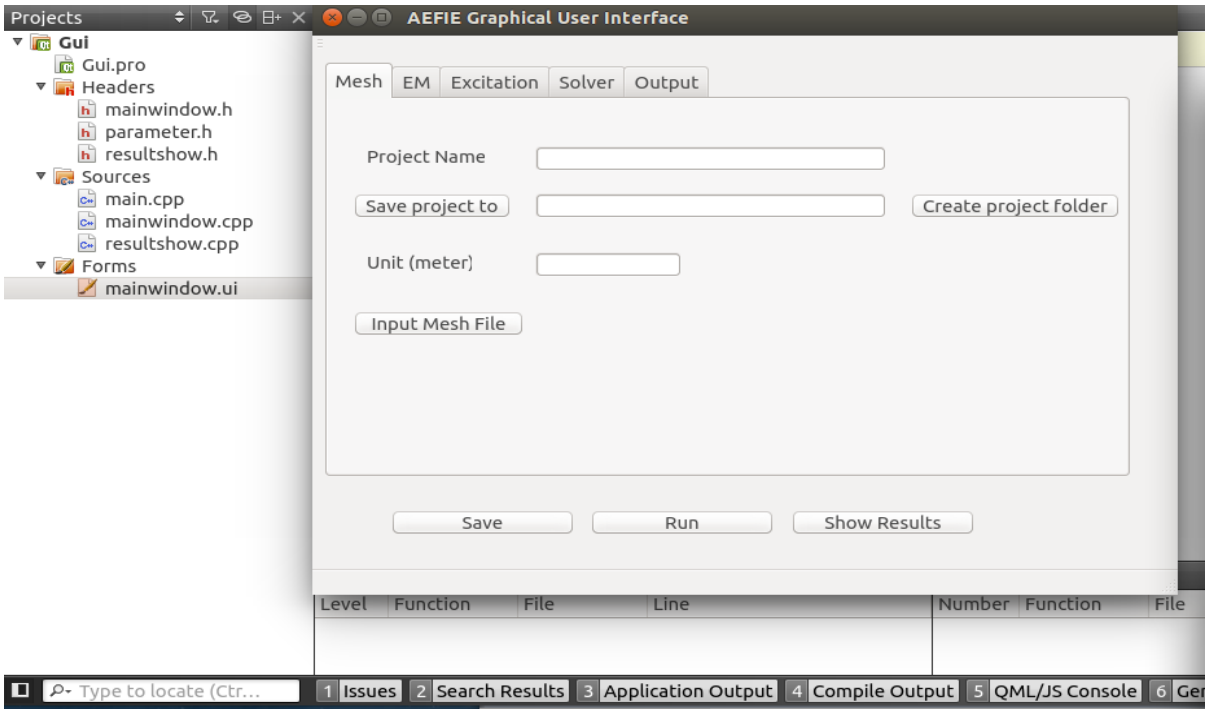

Figure 6-1 Function to locate the project directory

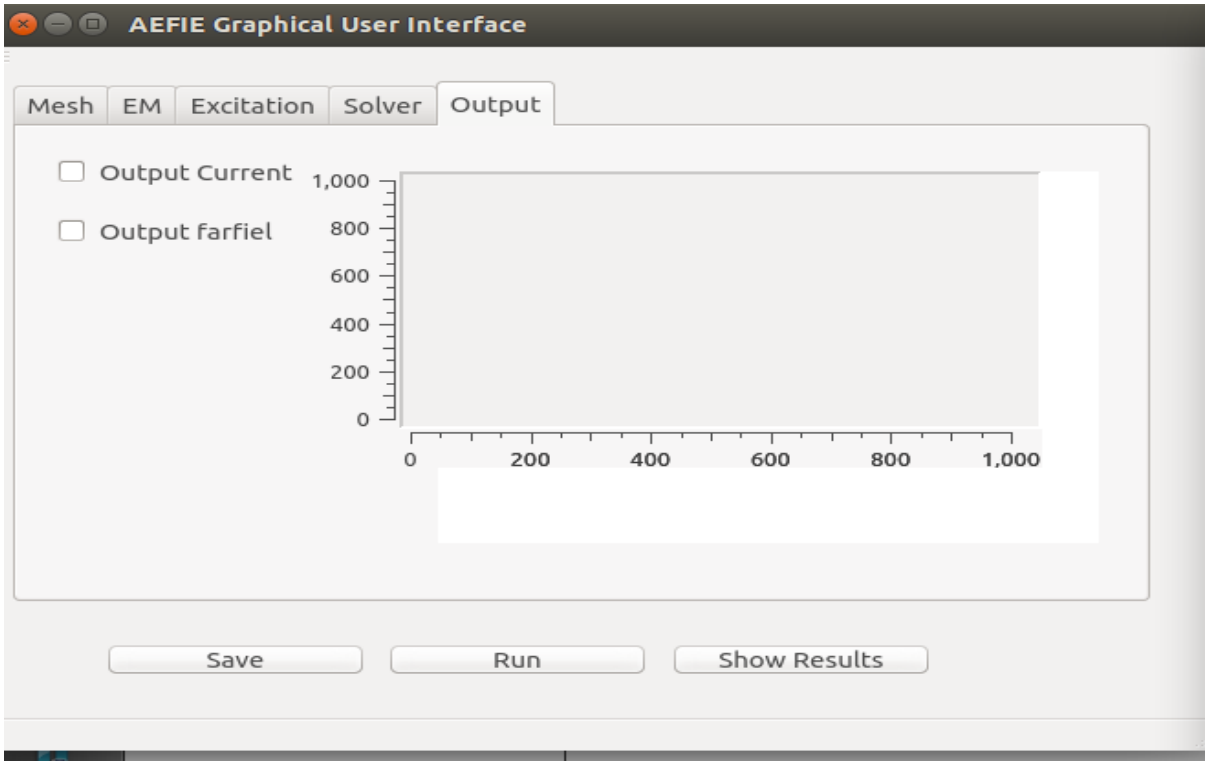

Figure 6-2 Function to plot out the output results

Creating the parameter file is accomplished and the Qwt package used to show outcome results. Linking the GUI and existing code is the next step. Creating three-dimensional view of the mesh file will be the final task.

6.2 Instructions for using the GUI

1. Choose the location of program folder and naming it according to the input project name
2. Select the mesh file for process and click “Input mesh file” button
3. Fill in all the required blanks
4. Click on the “Save” button
5. Click on the “Run” button upon success
6. Click on the “Show Results” button, and a new window will appear with output plots

7. Conclusion

Surface integral equations are useful to model full wave electromagnetic problems. Augmented SIEs can generally solve low frequency breakdown problems associated with EFIE operator. However, it is suggested from simulation results that at low frequency, there are still low frequency inaccuracies because of not being able to capture inductive behaviors of the circuit elements.

In future work, in order to increase the accuracy of modeling a certain geometry, smaller mesh size is required. Meanwhile, it might not be practical for the computer to handle the data with the same algorithm. A potential area of interest is a fast algorithm to accelerate the computation and maintain reasonable accuracy.

References

[1] W. C. Chew, M. S. Tong, B. Hu, *Integral Equation Methods for Electromagnetic and Elastic Waves*, Arizona, Morgan & Claypool Publishers, 2009.

[2] Zhi Guo Qian and W. C. Chew, "A quantitative study on the low frequency breakdown of EFIE," *Comm. Comp. Phys.,* vol. 50, no. 5, pp. 1159-1162, 2008.

[3] Weng Cho Chew, Zhi Guo Qian, Li J. Jiang and Y. P. Chen, "An augmented electric field integral equation for layered medium Green's function," *IEEE Transactions on Antennas and Propagation*., vol. 59, no. 3, pp. 960-968, 2011.

Appendix A: Source Code of GUI

1. Mainwindow.h

```
#Ifndef MAINWINDOW_H
#define MAINWINDOW_H
#include <QMainWindow>
#include<QFileDialog>
#include<QTextStream>
#include<QMessageBox>
#include<QDir>
#include<QString>

#include<QDebug>
#include<QTextStream>
#include<QApplication>
#include<QFileDialog>
#include<QTextStream>
#include<QMessageBox>
#include<QDir>
#include<QString>
#include<QFile>
#include<QDebug>
#include<QTextStream>
#include <QApplication>
#include <qmath.h>
#include <QVector>
#include <qwt_plot.h>
#include <qwt_plot_curve.h>
#include <qwt_plot_magnifier.h>
#include <qwt_plot_panner.h>
#include <qwt_legend.h>
#include "parameter.h"


namespace Ui {
class MainWindow;
}

class MainWindow : public QMainWindow
```

```
{
    Q_OBJECT

public:
    explicit MainWindow(QWidget *parent = 0);
    ~MainWindow();
    void writefile();

private slots:

    void on_SaveButton_clicked();

    void on_RunButton_clicked();

    void on_ExitButton_clicked();

    void on_pushButton_clicked();

    void on_pushButton_2_clicked();

    void on_lineEdit_3_textChanged();


    void on_lineEdit_textEdited(const QString &arg1);

    void on_pushButton_3_clicked();

    void on_lineEdit_11_textEdited(const QString &arg1);

    void on_lineEdit_19_textEdited(const QString &arg1);

    void on_lineEdit_20_textEdited(const QString &arg1);

    void on_checkBox_clicked();

    void on_checkBox_2_clicked();

    void on_checkBox_3_clicked();
```

```
    void on_checkBox_4_clicked();

    void on_checkBox_5_clicked();

    void on_checkBox_8_clicked();

    void on_checkBox_6_clicked();

    void on_checkBox_7_clicked();

    void on_checkBox_9_clicked();

    void on_checkBox_11_clicked();

    void on_checkBox_13_clicked();

    void on_checkBox_10_clicked();

    void on_checkBox_12_clicked();

    void on_checkBox_14_clicked();

    void on_checkBox_15_clicked();

    void on_checkBox_16_clicked();

    void on_checkBox_17_clicked();

    void on_checkBox_18_clicked();

private:
    Ui::MainWindow *ui;
    parameter myparameter;
};

#endif // MAINWINDOW_H
```

2. Mainwindow.cpp

```
#include "mainwindow.h"
#include "ui_mainwindow.h"
#include "mainwindow_2.h"

MainWindow::MainWindow(QWidget *parent) :
    QMainWindow(parent),
    ui(new Ui::MainWindow)
{
    ui->setupUi(this);
}

MainWindow::~MainWindow()
{
    delete ui;
}

void MainWindow::writefile()
{
    QFile mFile(myparameter.mesh_project_name+".para");

    if(!mFile.open(QFile::WriteOnly | QFile::Text))
    {
        qDebug() <<"Could not open file for writing";
        return;
    }
    QTextStream out(&mFile);
    //out<<"Hello world";
    out<<"PROJECTNAME:              ";
    out<<myparameter.mesh_project_name<<'\n';
    out<<"MESHUNIT:                 ";
    out<<myparameter.mesh_unit<<'\n';
    out<<"#FREQUENCYSWEEP:          ";
    out<<myparameter.frequency_lower_bound<<"
"<<myparameter.frequency_higher_bound<<"              "<<myparameter.number_of_frequency<<'\n';

    out<<"BACKGROUND:               \n";
    out<<QString::number(myparameter.background_medium_eps_r.toFloat(),'f',6)
            <<"     "<<QString::number(myparameter.background_medium_eps_i.toFloat(),'f',6)
```

```
            <<"      "<<QString::number(myparameter.background_medium_mu_r.toFloat(),'f',6)<<"
"<<QString::number(myparameter.background_medium_mu_i.toFloat(),'f',6)
                <<"      "<<QString::number(myparameter.background_medium_sigma.toFloat(),'e',6)<<'\n';
    out<<"EMPARAS:                  1\n";
    out<<"                          "<<QString::number(myparameter.medium_eps_r.toFloat(),'f',6)
       <<"      "<<QString::number(myparameter.medium_eps_i.toFloat(),'f',6)
    <<"      "<<QString::number(myparameter.medium_mu_r.toFloat(),'f',6)
    <<"      "<<QString::number(myparameter.medium_mu_i.toFloat(),'f',6)
       <<"      "<<QString::number(myparameter.medium_sigma.toFloat(),'f',1)
          <<"      "<<QString::number(myparameter.medium_thickness.toFloat(),'g',2)<<'\n';

    out<<"SOLVER:                   ";
    out<<myparameter.solver<<'\n';
    out<<"SOLVERMETHOD:             ";
    out<<myparameter.solver_method<<'\n';
    out<<"ACCURACYLEVEL:            ";
    out<<myparameter.accuracy_level;
    out<<"EXCITATIONTYPE:           ";
    out<<myparameter.excitation_type;
    out<<"PLANEWAVE:                ";
    out<<ui->lineEdit_16->text()<<"             "<<ui->lineEdit_18->text()<<"
"<<ui->lineEdit_21->text()<<'\n';
    out<<"PLANEWAVEOBS:             ";
    out<<ui->lineEdit_25->text()<<"             "<<ui->lineEdit_24->text()<<'\n';
    out<<"                          "<<ui->lineEdit_23->text()<<"
"<<ui->lineEdit_22->text()<<'\n';
    out<<"                          "<<ui->lineEdit_12->text()<<"
"<<ui->lineEdit_17->text()<<'\n';
    out<<"POINTSOURCE:              ";
    out<<"                          "<<ui->lineEdit_26->text()<<"
"<<ui->lineEdit_29->text()<<"           "<<ui->lineEdit_30->text()<<'\n';
    out<<"                          "<<ui->lineEdit_27->text()<<"
"<<ui->lineEdit_32->text()<<"           "<<ui->lineEdit_31->text()<<'\n';


    out<<"NEARFIELDOBS:         3";
    out<<"                          "<<ui->lineEdit_40->text()<<"
"<<ui->lineEdit_34->text()<<"           "<<ui->lineEdit_28->text()<<'\n';
```

```
        out<<"                              "<<ui->lineEdit_39->text()<<"
"<<ui->lineEdit_38->text()<<'\n';
        out<<"                              "<<ui->lineEdit_36->text()<<"
"<<ui->lineEdit_35->text()<<'\n';
        out<<"                              "<<ui->lineEdit_37->text()<<"
"<<ui->lineEdit_33->text()<<'\n';

        out<<"GMRESPARAS:                ";
        out<<"                              "<<ui->lineEdit_42->text()<<"
"<<ui->lineEdit_45->text()<<"               "<<ui->lineEdit_41->text()<<'\n';

        out<<"FMAPARAS:                  -1          ";
        out<<ui->lineEdit_44->text()<<"          "<<ui->lineEdit_46->text()<<"
"<<ui->lineEdit_43->text()<<'\n';

        out<<"NUMBEROBJECTS:           ";
        out<<ui->lineEdit_47->text()<<'\n';

        out<<"FMAOBJECTS:                "<<ui->lineEdit_49->text()<<'\n'<<"                0";

        mFile.flush();
        mFile.close();
}


void MainWindow::on_SaveButton_clicked()
{
        myparameter.mesh_unit=ui->lineEdit->text().toDouble();
        //Medium Page
        myparameter.background_medium_eps_r=ui->lineEdit_4->text();
        myparameter.background_medium_eps_i=ui->lineEdit_6->text();
        myparameter.background_medium_mu_r=ui->lineEdit_8->text();
        myparameter.background_medium_mu_i=ui->lineEdit_9->text();
        myparameter.background_medium_sigma=ui->lineEdit_15->text();
        myparameter.medium_eps_r=ui->lineEdit_5->text();
        myparameter.medium_eps_i=ui->lineEdit_7->text();
        myparameter.medium_mu_r=ui->lineEdit_10->text();
        myparameter.medium_mu_i=ui->lineEdit_13->text();
        myparameter.medium_sigma=ui->lineEdit_14->text();
```

```
    //Excitation page
    myparameter.frequency_lower_bound=ui->lineEdit_11->text();
    myparameter.frequency_higher_bound=ui->lineEdit_19->text();
    myparameter.number_of_frequency=ui->lineEdit_20->text();
    //Solver page
    myparameter.accuracy_level=ui->spinBox->value();




    //Solver II page
    ui->lineEdit->setText("load");
    //save to parameter file
    if (1==QDir::setCurrent(myparameter.home_directory+'/'+myparameter.mesh_project_name))
    {
        writefile();
    }
}

void MainWindow::on_RunButton_clicked()
{
    ui->lineEdit_2->setText("run");

}

void MainWindow::on_ExitButton_clicked()
{
    MainWindow_2 * result_current = new MainWindow_2;
    result_current->show();
}


void MainWindow::on_pushButton_clicked()
{
    QString filename=QFileDialog::getOpenFileName(
                this,
                tr("Open File"),
                "/Users/QQ"
                "All files (*.*);;Text File (*.txt);;Music file (*.mp3);;"
```

```
                        );

}

void MainWindow::on_pushButton_2_clicked()
{
    if (1==QDir::setCurrent(myparameter.home_directory)){
    QDir().mkdir(ui->lineEdit_3->text());
    //ui->lineEdit_2->setText("/Users/QQ");
    QMessageBox::information(0,"FYI","successfully created");
    }
}

void MainWindow::on_lineEdit_3_textChanged()
{
    myparameter.mesh_project_name=ui->lineEdit_3->text();
}



void MainWindow::on_pushButton_3_clicked()
{
    QString dir = QFileDialog::getExistingDirectory(this,tr("open directory"),"/Users/QQ",
                                                    QFileDialog::ShowDirsOnly
                                                    |QFileDialog::DontResolveSymlinks);
    ui->lineEdit_2->setText(dir);
    myparameter.home_directory=dir;
}




void MainWindow::on_checkBox_clicked()
{
    if(ui->checkBox->isChecked())
        myparameter.solver_method=1;
}
```

```
void MainWindow::on_checkBox_2_clicked()
{
    if(ui->checkBox_2->isChecked())
        myparameter.solver_method=2;
}

void MainWindow::on_checkBox_9_clicked()
{
    if(ui->checkBox_9->isChecked())
        myparameter.solver_method=3;
}

void MainWindow::on_checkBox_3_clicked()
{
   if(ui->checkBox_3->isChecked())
       myparameter.solver_method=4;
}

void MainWindow::on_checkBox_4_clicked()
{
    if(ui->checkBox_4->isChecked())
        myparameter.solver=1;
}

void MainWindow::on_checkBox_5_clicked()
{
    if(ui->checkBox_5->isChecked())
        myparameter.solver=2;
}

void MainWindow::on_checkBox_11_clicked()
{
    if(ui->checkBox_11->isChecked())
        myparameter.solver=3;
}

void MainWindow::on_checkBox_13_clicked()
{
    if(ui->checkBox_13->isChecked())
```

```
        myparameter.solver=4;
}

void MainWindow::on_checkBox_7_clicked()
{
    if(ui->checkBox_7->isChecked())
        myparameter.solver=5;
}

void MainWindow::on_checkBox_10_clicked()
{
    if(ui->checkBox_10->isChecked())
        myparameter.solver=6;
}

void MainWindow::on_checkBox_12_clicked()
{
    if(ui->checkBox_12->isChecked())
        myparameter.solver=7;
}

void MainWindow::on_checkBox_14_clicked()
{
    if(ui->checkBox_14->isChecked())
        myparameter.excitation_type=1;
}

void MainWindow::on_checkBox_15_clicked()
{
    if(ui->checkBox_15->isChecked())
        myparameter.excitation_type=2;
}

void MainWindow::on_checkBox_16_clicked()
{
    if(ui->checkBox_16->isChecked())
        myparameter.observation_coordinate=1;
}
```

```
void MainWindow::on_checkBox_17_clicked()
{
    if(ui->checkBox_17->isChecked())
        myparameter.observation_coordinate=2;
}

void MainWindow::on_checkBox_18_clicked()
{
    if(ui->checkBox_18->isChecked())
        myparameter.observation_coordinate=3;
}
```